

Ultrafast Intramolecular Electron Transfer in Peripherally Ruthenated Zinc Tetraarylporphyrins

Mark H. Wall, Jr.,[#] Seiji Akimoto, Tomoko Yamazaki, Nobuhiro Ohta, Iwao Yamazaki,*
Takuya Sakuma,[†] and Hiroaki Kido[†]

Department of Molecular Chemistry, Graduate School of Engineering, Hokkaido University, Sapporo 060-8628

[†]Department of Industrial Chemistry, College of Engineering, Nihon University, Koriyama 963

(Received December 7, 1998)

Ultrafast fluorescence quenching has been examined for 5-pyridyl-10,15,20-triphenylporphinatozinc (ZnP), which is coordinatively linked to ruthenium complex (oxo-acetato-bridged-triruthenium ions) (Ru), and for its derivatives having cyanopyridyl groups (Ru1) or 4-(*N,N*-dimethylamino)pyridyl groups (Ru2). The fluorescence for these peripherally elaborated zinc tetraarylporphyrins are > 99% quenched relative to ZnP. Fluorescence decays were measured in different solvents using the technique of femtosecond fluorescence up-conversion for these three compounds: ZnP–Ru⁺, ZnP–Ru⁺–Ru1⁺, and ZnP–Ru⁺–Ru2⁺. The fluorescence lifetime for ZnP* (τ_f = 1.7–1.8 ns in ZnP monomer) is dramatically decreased by the linkage of ruthenium moieties to the periphery of ZnP; τ_f = 460–530 fs for ZnP*–Ru⁺, τ_f = 380–400 fs for ZnP–Ru⁺–Ru1⁺, and τ_f = 300–380 fs for ZnP–Ru⁺–Ru2⁺. This fluorescence quenching behavior is in accord with a semiempirical estimation of the free energy for electron transfer from ZnP* to Ru⁺. Thus the ultrafast fluorescence quenching process in these molecules is attributed to an intramolecular electron transfer governed by the following equations: ZnP*–Ru⁺ → ZnP⁺–Ru⁰ and ZnP*–Ru⁺–Ru1⁺ (or Ru2⁺) → ZnP⁺–Ru⁰–Ru1⁺ (or Ru2⁺).

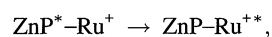
Photochemical processes such as electron transfer and excitation energy transfer are expected to occur very rapidly in organized molecular systems in which donor (D) and acceptors (A) are located within close proximity and optimal orientation. Donor moieties in these molecules can be coupled to adjacent acceptor moieties with relatively strong interaction, resulting in the possibility of ultrafast photochemical reaction. Several examples have been reported for intramolecular electron transfer in bridged donor/acceptor molecules where the reaction time scale is less than 1 ps.^{1–3} An overview of recent experiments and fundamental problems involved in bridged D/A systems has recently been presented by Barbara, Meyer, and Ratner.⁴ It has been pointed out in these experimental and theoretical studies that electron transfer rates are relatively insensitive to solvation dynamics and that the reactant nuclear vibrations play an essential role in promoting rapid intramolecular electron transfer. Further studies are required before a fully consistent picture is available for such an ultrafast electron transfer.

Kido and Ito have synthesized dimers and trimers of pyrazine-bridged oxo-acetato-bridged triruthenium (Ru–pyrazine–Ru and Ru–pyrazine–Ru–pyrazine–Ru).^{5,6} Rapid electron transfer (10^9 – 10^{12} s^{−1}) between Ru groups has been predicted for these dimers and trimers from analyses of the redox potential and infrared spectroscopic characteristics.⁷ However, for the fast electron transfer process to be con-

firmed in these dimers and trimers, a time-resolved spectroscopic measurement is required. In connection with this problem, we have studied ultrafast fluorescence quenching on related molecules using a fluorescence up-conversion technique. These molecules were prepared by modifying Ru–pyrazine–Ru and Ru–pyrazine–Ru–pyrazine–Ru dimer and trimers. The present study is concerned with three molecules, as shown in Fig. 1, in which the Ru moieties are linked to the periphery of zinc tetraarylporphyrin (ZnP) at the *meso* position. Specifically, we investigate the fluorescence behavior in a ZnP–Ru⁺ dyad and two ZnP–Ru⁺–Ru⁺ triads (ZnP–Ru⁺–Ru1⁺ and ZnP–Ru⁺–Ru2⁺), where Ru1⁺ and Ru2⁺ contain electron withdrawing cyanopyridyl groups and electron-releasing dimethylamino groups, respectively. Preliminary experiments have shown that following photoexcitation of the dyads and triads, the fluorescence for these peripherally elaborated zinc tetraarylporphyrins are > 99% quenched relative to ZnP.

In this study, we have measured the fluorescence lifetimes of the dyads and triads in the femtosecond time regime using a fluorescence up-conversion method, and determined the quenching rate constants in different solvents. We will discuss the ultrafast fluorescence quenching phenomenon from the viewpoint of two possible reaction processes:

(1) the excitation energy transfer



(2) the electron transfers

[#] Present address: Department of Chemistry, The University of Idaho, Moscow, ID 83844, U. S. A.

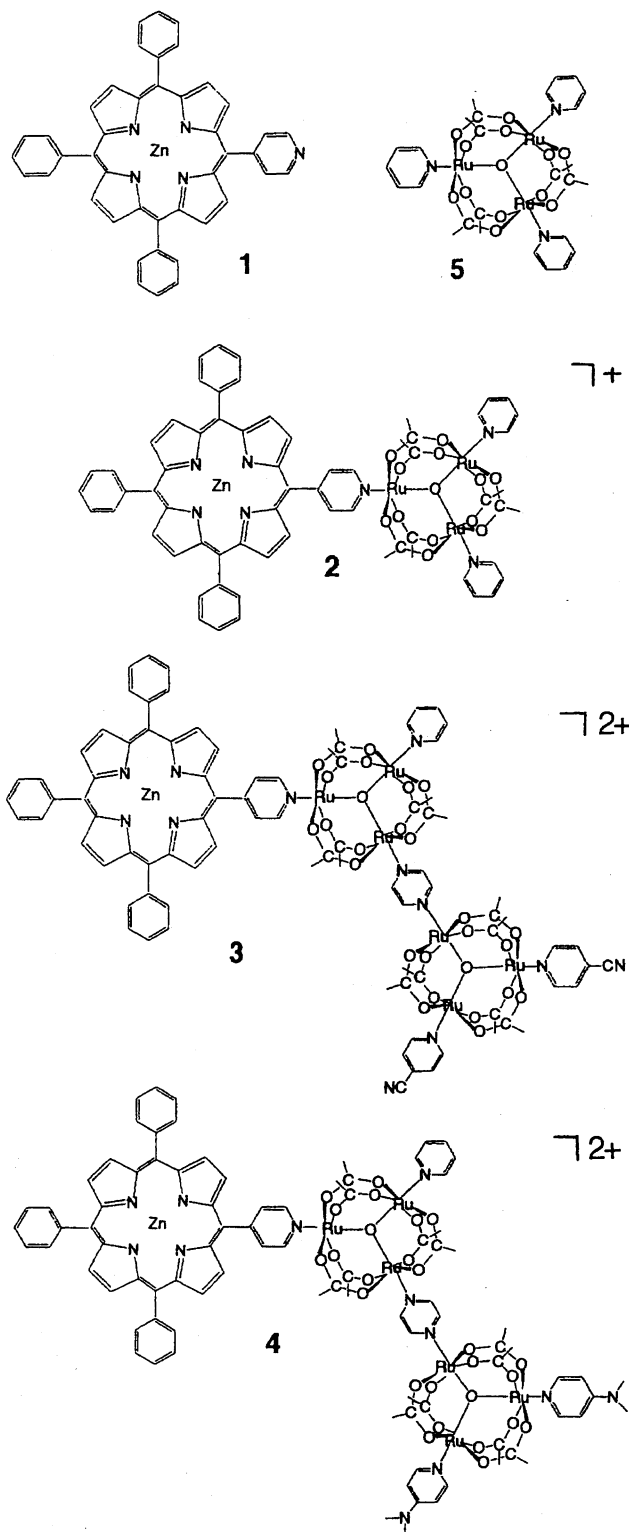
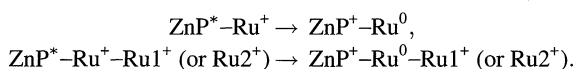


Fig. 1. Structural formulas of zinc tetraarylporphyrin–ruthenium complexes.



We will present a discussion on the intramolecular excitation energy transfer based on an analysis of the spectral overlap between the ZnP^* (donor) fluorescence and the Ru^+

(acceptor) absorption. This will be followed by a discussion of intramolecular electron transfer based on an analyses of the free energy of the redox reactions in different solvents. We will reach a conclusion that the predominant pathway responsible for the fluorescence quenching in the dyad and triads is intramolecular electron transfer.

Experimental

The Zn porphyrin monomer, Ru monomer and zinc tetraarylporphyrin–ruthenium dyads and triads in this study are ZnP , **1**, $[(\text{ZnP})(\text{py})\text{Ru}_3(\text{py})_2]\text{PF}_6$, **2**, $[(\text{ZnP})(\text{py})\text{Ru}_3(\text{pz})\text{Ru}_3(\text{cpy})_2](\text{PF}_6)_2$, **3**, $[(\text{ZnP})(\text{py})\text{Ru}_3(\text{pz})\text{Ru}_3(\text{dmpy})_2](\text{PF}_6)_2$, **4**, and $\text{Ru}_3(\text{py})_3$, **5**, where ZnP = 5-pyridyl-10, 15, 20-triphenylporphinatozinc, Ru_3 = $\text{Ru}_3(\mu_3\text{-O})(\mu\text{-CH}_3\text{COO})_6$ moiety, py = pyridine, pz = pyrazine, cpy = 4-cyanopyridine, and dmpy = 4-(*N,N*-dimethylamino)pyridine. These compounds were synthesized by the methods reported previously^{5,6} as microcrystalline powder involving a counter ion PF_6^- . The samples were dissolved in different solvents with concentrations of $(1-5) \times 10^{-5}$ M (1 M = 1 mol dm⁻³).

Absorption and steady-state fluorescence spectra were measured with a JASCO Ubest-50 spectrophotometer and a JASCO FP-770F spectrofluorometer, respectively. Picosecond fluorescence decay measurements were obtained with a time-correlated, single-photon timing method on an instrument previously described.⁸ Femtosecond fluorescence decay curves were measured by means of a fluorescence up-conversion method. The details of this system was described in previous papers.^{9,10} Briefly, the pump-probe protocol utilized the second harmonics (420 nm, 0.7 nJ pulse⁻¹) from a Ti:Sapphire laser (840 nm, < 150 fs FWHM, 76 MHz, 10 nJ pulse⁻¹) to excite the ZnP moiety into the second excited singlet state, S_2 . The fundamental laser pulse (840 nm) as a probe pulse and the fluorescence from the photoexcited sample (at 610 nm) were tightly focused in a point on a BBO crystal to produce a sum-frequency light. By changing the time difference between the probe pulse and the excitation pulse with an optical delay line, a fluorescence time profile is obtained in 6.7 fs per channel. To avoid polarization effects, the angle between the polarizations of excitation and probe beams were set to the magic angle by using a $\lambda/2$ plate. The pulse width of the instrumental response function was 250 fs (FWHM). Fluorescence lifetimes were determined by the curve fitting method for convoluted curves. All measurements were carried out at room temperature under aerobic conditions.

Results

Figure 2 shows the absorption spectra of ZnP , **1**, Ru , **5**, $\text{ZnP}-\text{Ru}^+$, **2**, and $\text{ZnP}-\text{Ru}^+-\text{Ru}1^+$, **3**, in toluene solution. The absorption spectrum of **1** is characterized by an intense band centered at 422 nm known as the Soret band and two weak absorption bands centered at 552 and 600 nm known as the Q(0,1) and Q(0,0) bands, respectively. The absorption spectrum of **5** shows a broad absorption band centered at 680 nm. The absorption spectrum of $\text{ZnP}-\text{Ru}^+$ approximates a superposition of absorbances of the individual ZnP and Ru groups with small shifts to lower energy relative to the absorbances of **1** and **5** for the absorption bands in the near IR region. Similar behavior is observed for the absorption spectrum of **3** which is roughly approximated by a superposition of the absorption spectra of ZnP and two Ru^+ groups. The spectral shift, observed for **3** relative to **2**, in the lowest energy absorption band may be attributed to the differences

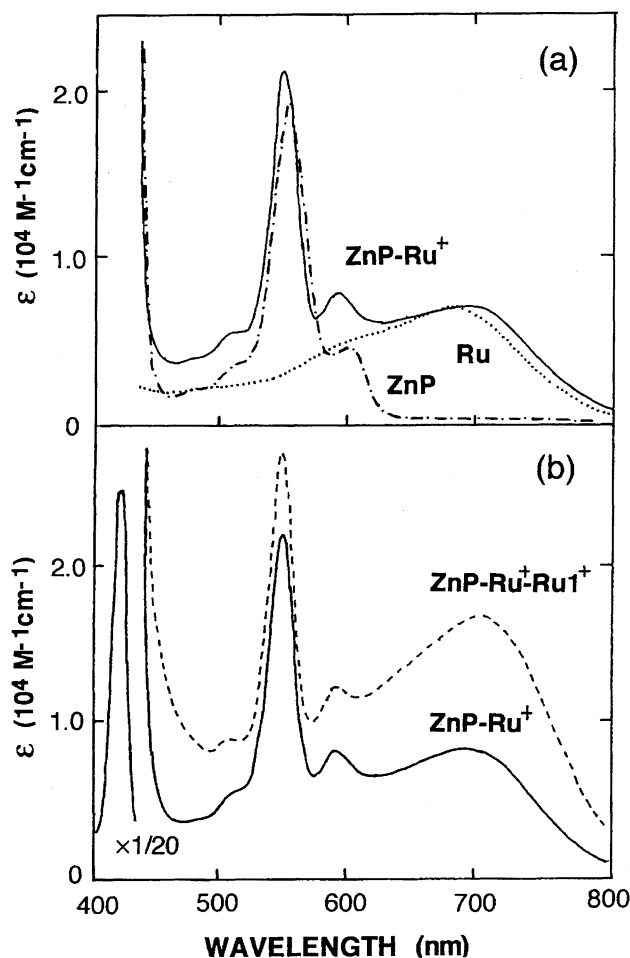


Fig. 2. Absorption spectra of ZnP, **1**, Ru, **5**, ZnP-Ru⁺, **2**, and ZnP-Ru⁺-Ru1⁺, **3**, in toluene; (a) the spectrum of ZnP-Ru⁺ exhibits approximately a superposition of the spectra of ZnP and Ru, and (b) the spectrum of ZnP-Ru⁺-Ru1⁺ shows a two-fold increase in intensity in the Ru⁺ (or Ru1⁺) absorption region.

between the Ru⁺ and Ru1⁺ and weak electronic interaction between these groups.

The fluorescence spectrum of **1** in toluene is shown in Fig. 3. The spectrum is typical of zinc tetraphenylporphyrin exhibiting two vibrational bands centered at 595 and 645 nm. In contrast to the fluorescence observed for **1**, no fluorescence emissions were detected for **2**, **3**, and **4** by standard steady-state fluorimeter. This indicates that upon attachment of the Ru group(s) to the periphery of ZnP, there is a > 99% quenching of the ZnP fluorescence. The fluorescence decay curves of **1**, **2**, and **3** are presented in Fig. 4. Each fluorescence decay curve was obtained using an excitation wavelength of 420 nm and monitored at 610 nm. The fluorescence decay curve for **1** was measured by a picosecond time correlated, single-photon timing method and the decay curves for **2** and **3** were measured using the femtosecond fluorescence up-conversion method. Plots of the peak intensity of the decay curves as a function of monitoring wavelength for **2**–**4** (not shown) gave a spectral profile identical to the steady state emission spectrum of **1**. This indicates that, the fluorescence detected

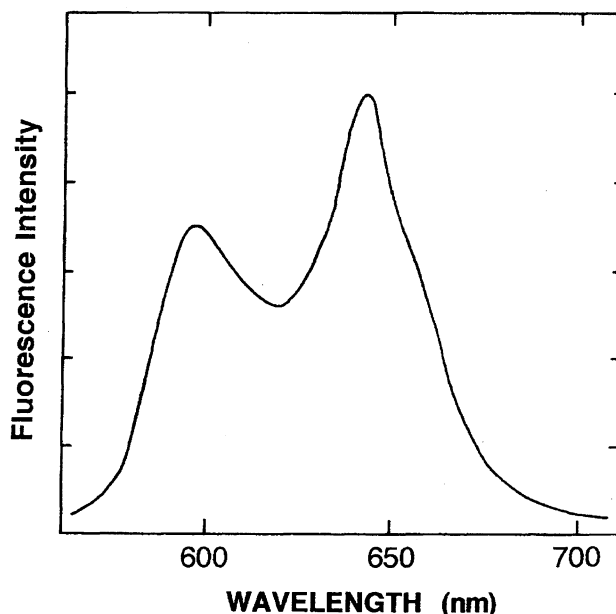


Fig. 3. Fluorescence spectrum of ZnP, **1**, in toluene. The excitation wavelength is 420 nm.

for **2**, **3**, and **4** as shown in Fig. 4 is emission from a locally excited state of the ZnP moiety. The fluorescence lifetimes of **1**–**4** in the solvents of toluene, tetrahydrofuran and benzonitrile are summarized in Table 1. The decay of **1** in each of the different solvents can be fit to a single exponential with lifetimes of 1.7–1.8 ns. In contrast, the fluorescence decay curves observed for **2**–**4** show single exponential decays with significantly shorter lifetimes. In each of the different solvents, the lifetimes for **2** were in the range of 460–530 fs, for **3** the lifetimes were in the range of 380–400 fs, and for **4** the lifetimes ranged in 300–380 fs.

The experimental results are summarized as follows: (1) the fluorescence lifetime is decreased by a factor of three thousand upon attachment of the Ru⁺ (Ru⁺-Ru1⁺ or Ru⁺-Ru2⁺) to the periphery of ZnP; (2) the fluorescence quenching rate constant, k_q ($=\tau_f^{-1}$), is relatively insensitive to changes in solvent polarity with values in the range of $2\text{--}3 \times 10^{12} \text{ s}^{-1}$; and (3) the k_q value increases in going from **2** to **3** and **4** in each of the different solvents.

Discussion

The ultrafast fluorescence quenching in ZnP^{*}-Ru⁺ and ZnP^{*}-Ru⁺-Ru1⁺ (and -Ru2⁺) may be understood as resulting from new decay processes introduced by the attachment of the Ru moiety (i.e., Ru⁺, Ru⁺-Ru1⁺ or Ru⁺-Ru2⁺) to the periphery of ZnP. These new decay processes include intramolecular energy transfer and electron transfer from ZnP^{*} to the adjacent Ru moiety.

Intramolecular energy transfer may occur between ZnP^{*} and the adjacent Ru moiety due to the close proximity of these two groups (11.8 Å center-to-center distance) and the large spectral overlap between ZnP^{*} (donor) fluorescence (Fig. 3) and the Ru (acceptor) absorption (Fig. 2). According to the Förster mechanism, the energy transfer rate k_E is proportional

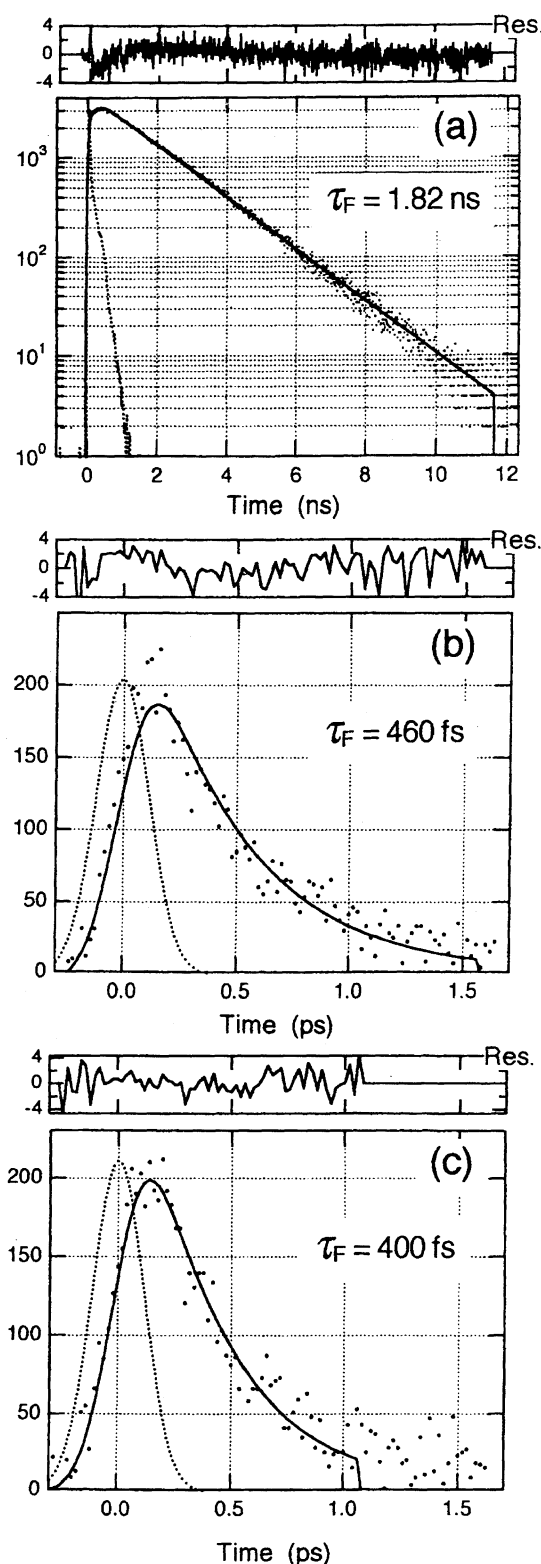


Fig. 4. Fluorescence decay curves of (a) ZnP, **1**, (b) ZnP–Ru⁺, **2**, and (c) ZnP–Ru⁺–Ru1⁺, **3**, in toluene; (a) measured with a picosecond time-correlated, single-photon counting method, and (b) measured with a fluorescence up-conversion method. The excitation laser wavelength is 420 nm.

to the spectral overlap as follows,¹¹

$$k_E \propto \frac{1}{n^4} \int_0^\infty \frac{F_d(\nu)\epsilon_a(\nu)}{\nu^4} d\nu, \quad (1)$$

where $F_d(\nu)$ is the fluorescence intensity of the donor in the wavenumber range ν to $\nu+d\nu$ with the total integrated intensity normalized to unity, $\epsilon_a(\nu)$ is the extinction coefficient of the acceptor and n is the refractive index of solvent. Therefore, the spectral overlap can serve as a sensitive probe for establishing energy transfer in ZnP^{*}–Ru⁺. Spectral shifts are observed for the ZnP fluorescence and the Ru⁺ absorption spectra with changes in solvent polarity. This results in significant changes to the spectral overlap between donor emission and acceptor absorption. The calculated spectral overlaps in toluene, tetrahydrofuran and benzonitrile are listed in Table 2. For the weakly and non-coordinating solvents, tetrahydrofuran and toluene, the calculated spectral overlap in toluene is 0.55 of the calculated overlap for tetrahydrofuran. However, it was observed that the fluorescence lifetimes in tetrahydrofuran and toluene were nearly equal. Furthermore, the lifetime observed in benzonitrile is longer than the lifetime in toluene. Thus the observed solvent dependence of k_q disagrees with the theoretical expectation. It can therefore be postulated that energy transfer can not be the exclusive mechanism responsible for the enhanced decay of porphyrin fluorescence observed in ZnP^{*}–Ru⁺.

It is well known that oxo-acetato-bridged triruthenium complexes [Ru₃(μ₃-O)(μ-CH₃COO)₆L₃]ⁿ⁺ (L = neutral ligands) are redox active and undergo reversible, multistep one-electron processes from [Ru₃(IV, IV, III)]³⁺ to [Ru₃(II, II, II)]²⁻.¹² The one-electron redox reactions were confirmed for the compounds under investigation here by cyclic voltammetric measurements.⁶ For molecules **1**–**5** in CH₂Cl₂, the reversible redox processes occur at +0.8 V vs. SCE for ZnP^{0/+} and at ca. 0 V region for [Ru₃(III, III, III/III, III, II)]^{+/0}; –0.20 V for **2**, –0.09 V (ZnP–Ru^{+/0}–Ru1⁰), +0.06 V (ZnP–Ru⁺–Ru1^{+/0}) for **3**, and –0.04 V (ZnP–Ru^{+/0}–Ru2⁺), –0.24 V (ZnP–Ru⁰–Ru2^{+/0}) for **4**. Since ZnP gains ca. 2.1 eV (0–0 band) upon photoexcitation, $E_{1/2}$ for *ZnP^{0/+} is expected to be ca. –1.3 V. This is significantly more negative than $E_{1/2}$'s of the Ru cores and thus, it is thermodynamically favorable for electron transfer to occur between the ZnP^{*} and the adjacent Ru moieties in **2**–**4**.

According to the theory of photoinduced electron transfer kinetics,^{13,14} the reaction rate depends on several factors. These factors include the magnitude of the electronic coupling between the electron donor and acceptor (which also includes a distance and orientation dependence), the free energy gap between initial and final states, and the coordination of solvent molecules surrounding the electron donor and acceptor. For weakly electronically coupled donor–acceptor systems, the following equation is commonly used for the rate constant k_{ET} ,

$$k_{ET} = \left(\frac{2\pi}{\hbar} \right) V^2 \exp \left\{ -\frac{(\Delta G^\circ + \lambda)^2}{4\lambda k_B T} \right\}, \quad (2)$$

where V represents the electronic coupling between donor

Table 1. Fluorescence Lifetimes (τ_f in ps Unit) and Decay Rate Constants (k_q in 10^{12} s^{-1} Unit)

Compounds	Toluene		THF		Benzonitrile	
	τ_f	k_q	τ_f	k_q	τ_f	k_q
1 ZnP	1820	5.5×10^{-4}	1660	6.0×10^{-4}	1650	6.0×10^{-4}
2 ZnP–Ru ⁺	0.46	2.2	0.46	2.2	0.53	1.9
3 ZnP–Ru ⁺ –Ru1 ⁺	0.40	2.5	0.40	2.5	0.38	2.6
4 ZnP–Ru ⁺ –Ru2 ⁺	0.38	2.6	0.33	3.0	0.30	3.3

Table 2. Relative Spectral Overlap and Fluorescence Lifetimes of ZnP⁺–Ru⁺

	Solvents		
	Toluene	THF	Benzonitrile
Magnitude of spectral overlap ^{a)}	0.55	1	0.75
Lifetime (ps)	0.46	0.46	0.53

a) The relative values normalized to the value in THF.

and acceptor, ΔG° is the free energy of charge separation, k_B is the Boltzman constant, λ ($= \lambda_i + \lambda_0$) is the reorganization energy which includes components from changes in bond lengths (λ_i) and from changes in solvent orientation coordinates between the initial and final states (λ_0). In this expression, the activation energy is given in the form of $\Delta G^\ddagger = (\Delta G^\circ + \lambda)^2 / 4\lambda$, and the reorganizational energy is usually expressed by the following equation,

$$\lambda_0 = (\Delta e)^2 \left\{ \frac{1}{2a_D} + \frac{1}{2a_A} - \frac{1}{r_{DA}} \right\} \left\{ \frac{1}{\epsilon_\infty} - \frac{1}{\epsilon_0} \right\}, \quad (3)$$

where a_D and a_A are the radii of the donor and acceptor respectively, r_{DA} is the distance between donor and acceptor, and ϵ_∞ and ϵ_0 are the optical frequency and zero frequency dielectric constants of the solvent, and Δe is the amount of charge transferred. The free energy ΔG° can be written as

$$\Delta G^\circ = E_{D^+A^-} - E_{S1} = D_{ox} - A_{red} - E_{S1}, \quad (4)$$

where E_{S1} is the energy of the 0–0 transition between S_1 and S_0 states of ZnP, D_{ox} and A_{red} are respectively the half-wave potentials of one-electron oxidation of ZnP⁺ and the one-electron reduction of Ru⁺, which were measured by a cyclic voltammetry in CH₂Cl₂ solutions mentioned before. In many cases where electron transfer reactions are of a type of (D–A) \rightarrow (D⁺–A[–]), a correction term ΔG_S is involved in Eq. 4 for the effects of the solvent polarities as well as the Coulombic energy between the charged donor and acceptor. In the present case of the reaction (D–A⁺) \rightarrow (D⁺–A), however, ΔG_S can be neglected, presumably because the solvation effects in the reactant Ru⁺ and the product ZnP⁺ are similar to each other, and contribute little to ΔG° .

We have estimated from Eqs. 2, 3, and 4 the values of the free energy ΔG° and the exponential term of Eq. 2 $\exp(-\Delta G^\ddagger/k_B T)$ for compounds 2, 3, and 4 in various solutions. The results are summarized in Table 3. In the calculation of ΔG° , the D_{ox} – A_{red} values are taken from those obtained by a cyclic voltammetry presented earlier,⁶ and the E_{S1} values are taken from the absorption spectra and pre-

sented in Table 3. For the calculation of $\exp(-\Delta G^\ddagger/k_B T)$, we used the parameter values $a_D = a_A = 5 \text{ \AA}$, $r_{DA} = 12 \text{ \AA}$, $\epsilon_\infty = n^2$ (the square of the refractive index of solvent), and ϵ_s is the static dielectric constant of the solvent. The λ_i value was taken as 0.6 eV from a charge transfer reaction in a bridged donor/acceptor (porphyrin–quinone) system with similar geometry.¹⁵

From Table 3, it can be seen that, for the first step of electron transfer, ZnP⁺–Ru⁺ \rightarrow ZnP⁺–Ru⁰, the overall free energy of reaction ΔG° is sufficiently large (-1.1 — -1.2 eV) such that an effective photoinduced electron transfer can occur as exothermic reactions in all the cases of the compounds in various solutions. Particularly, one should note that the ΔG° value is almost constant irrespective of compounds and solvents. On the other hand, the quantity $\exp(-\Delta G^\ddagger/k_B T)$ relevant to the electron transfer rate (Eq. 2) is greatly changed depending on solvent and compound. The values for THF and benzonitrile solutions are fairly large and exhibit enhancement by linkage of Ru1⁺ or Ru2⁺. The value for toluene solution in turn is much smaller than those for THF and benzonitrile and, particularly it decreases in triads, contrary to the experimental result. Note that Eq. 3 for the reorganization energy (λ_0) due to changes in solvent orientation is a rather poor approximation in nonpolar solvents,¹⁵ and that the dielectric effect for the outer-sphere reorganizational energy is based on specific assumptions with respect to geometry of two spherical reactants and equilibration during the reaction. Besides this disagreement between theory and experiment with respect to the solvent effect, several examples have demonstrated that the rate of ultrafast intramolecular electron transfer is rather insensitive to environmental factors like solvent dielectric relaxation effects, as is shown below. Therefore, we might consider preferably the ultrafast fluorescence quenching under investigation as due to the intramolecular electron transfer.

Macpherson et al.² studied ultrafast photoinduced electron transfers in porphyrin (D) linked to a quinone (A) through a rigid bicyclic bridge. It was found that the intramolecular electron transfer occurs with rate constants of ca. 10^{12} s^{-1} irrespective of solvent and temperatures from 77 to 295 K. They reached a conclusion, from thermodynamic analyses of the electron transfer and its lack of dependence on environmental factors, that the rapid electron transfer is governed by intramolecular vibrations. Also Häberle et al.³ studied with molecular systems of cyclophane-bridged Zn-porphyrin (D)–quinone (A) with various derivatives in driving forces ranging from 0.2 to 1.3 eV, and found that the ultrafast charge separation occurs with a rate constant of

Table 3. Values of $E(S_1)$, $E_{\text{ox}} - E_{\text{red}}$, $-\Delta G^\circ$ and $\exp(-\Delta G^\ddagger/k_B T)$

	Compounds	$E(S_1)$ (eV)		
		Toluene	THF	Benzonitrile
2	ZnP*–Ru ⁺	2.09	2.08	2.06

The values taken from the absorption peak of ZnP in the lower energy side of Q band.

	Compounds	$E_{\text{ox}} - E_{\text{red}}$	$-\Delta G^\circ$ (eV)		
		eV	Toluene	THF	Benzonitrile
2	ZnP*–Ru ⁺	0.97	1.12	1.11	1.09
3	ZnP*–Ru ⁺ –Ru1 ⁺	0.92	1.17	1.16	1.14
4	ZnP*–Ru ⁺ –Ru2 ⁺	0.93	1.16	1.14	1.13

The values of $E_{\text{ox}} - E_{\text{red}}$ and $-\Delta G^\circ$ are taken for the first-step electron transfer, i.e., ZnP*–Ru⁺ → ZnP⁺–Ru⁰ and ZnP*–Ru⁺–Ru1⁺ (or –Ru2⁺) → ZnP⁺–Ru⁰–Ru1⁺ (or –Ru2⁺).

	Compounds	$\exp(-\Delta G^\ddagger/k_B T)$		
		Toluene	THF	Benzonitrile
2	ZnP*–Ru ⁺	0.0614	0.159	0.108
3	ZnP*–Ru ⁺ –Ru1 ⁺	0.0005	0.650	0.459
4	ZnP*–Ru ⁺ –Ru2 ⁺	0.0007	0.628	0.439

The values of $\exp(-\Delta G^\ddagger/k_B T)$ are taken for the first-step electron transfer, i.e., ZnP*–Ru⁺ → ZnP⁺–Ru⁰ and ZnP*–Ru⁺–Ru1⁺ (or –Ru2⁺) → ZnP⁺–Ru⁰–Ru1⁺ (or –Ru2⁺).

$(2\text{--}5) \times 10^{12} \text{ s}^{-1}$. The analysis confirms the predominance of intramolecular reorganization which is consistent with the absence of solvent dielectric relaxation effects on the rate of electron transfer. The present experimental results have offered an additional example of such ultrafast intramolecular electron transfer under the same situation as observed in previous studies.

Concluding Remarks

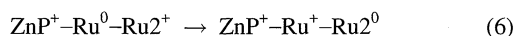
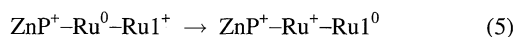
The present study has demonstrated that a zinc tetraporphyrin undergoes ultrafast fluorescence quenching by linkage of a triruthenium complex pendant; the rate constants of excitation quenching (k_q) are determined to be $(1.9\text{--}2.2) \times 10^{12} \text{ s}^{-1}$ in dyad (ZnP–Ru⁺) and $(2.5\text{--}3.3) \times 10^{12} \text{ s}^{-1}$ in triad (ZnP–Ru⁺–Ru1⁺ and –Ru2⁺), and the quenching rates are fairly constant irrespective of solvent. When the electron transfer is assumed to be responsible for these quenching processes, the increase of k_q in going from dyad to triad is in accord with the theoretical estimation of relative reaction rate based on thermodynamical redox potentials. Thus we assign preferably the quenching processes as due to the photoinduced electron transfer rather than the excitation transfer. In this assignment, however, the constant reaction rate in a particular compound in different solvents cannot be interpreted from the conventional electron transfer theory. This specific behavior may allow us to consider that the present molecular systems are in a situation similar to the cases of bridged Zn porphyrin–quinone systems^{2,3} and ADMA⁴ where intramolecular nuclear

vibrations play a predominant role in the reaction.

In the present study, ZnP was photoexcited at Soret band (420 nm) associated with the $S_2 \leftarrow S_0$ transition. Suppose that the internal conversion $S_2 \rightarrow S_1$ is extremely fast (less than 100 fs), the energy level in S_1 reached after the internal conversion contains vibrational excess energy of about 7000 cm^{-1} which is much larger than the largest estimated barrier for the electron transfer ca. 1500 cm^{-1} . Furthermore the measured characteristic times of electron transfer (300–500 fs) might be comparable with the time scale of the vibrational relaxation along the S_1 potential energy surface. In fact, recent experiments on excited-state dynamics of organic dye molecules in solution demonstrated that the vibrational relaxation and energy diffusion into solvents take place in picosecond time scales: Mokhtari, Chesnoy, and Laubereau¹⁶ studied a time-dependent broadening of the fluorescence bandwidth of Nile blue in methanol, and showed that the vibrational relaxation takes place with 4 ps time constant; and Martini and Hartland¹⁷ demonstrated that in hexamethyl indotricarbocyanine in organic solvents it occurs in 1.7–7.1 ps depending on solvent. If this is the case, the electron transfer in ZnP–Ru complexes may occur from a vibrationally hot state prepared by high energy excitation. In this case the semiclassical theory used for estimations of the reaction rates will not be applicable, and it provides us with a reason for some discrepancy between the experiment and the theory. In order to study the possibility of non-equilibrium electron transfer reaction, further experiments will be necessary concerning the vibrational relaxation process;

these will be made in future work.

One should note that in the triads the first step of electron transfer $\text{ZnP}^+-\text{Ru}^+-\text{Ru1}^+$ (or $-\text{Ru2}^+$) $\rightarrow \text{ZnP}^+-\text{Ru}^0-\text{Ru1}^+$ (or $-\text{Ru2}^+$) can be followed by the second-step electron transfer from Ru^0 to Ru1^+ or Ru2^+ , that is,



The present experiment based on fluorescence decay measurement for ZnP^* gives no information on this reaction step. The free energy estimation (the data is not shown) predicts that this reaction is possible in the Ru1 sequence (process 5), but not in the Ru2 sequence (process 6), because the state $\text{ZnP}^+-\text{Ru}^+-\text{Ru1}^0$ is further stabilized relative to the $\text{ZnP}^+-\text{Ru}^0-\text{Ru1}^+$ state in polar solvents like THF and benzonitrile, whereas the state $\text{ZnP}^+-\text{Ru}^+-\text{Ru2}^0$ is higher in energy than the $\text{ZnP}^+-\text{Ru}^0-\text{Ru2}^+$. In order to examine the second-step electron transfer, a transient absorption measurement is required which enables us to measure directly the spectra and the time courses of the final ion-pair species.

This work was financially supported in part by Japanese Society for the Promotion of Science Post-doctoral Fellowship to M.H.W., and by the Grant-in-Aids for Scientific Research from the Ministry of Education, Science, Sports and Culture to I. Y. (Nos. 09304056 and 09354008) and to H. K. (No. 8640726).

References

- 1 K. Tominaga, D. A. Kliner, A. E. Johnson, N. E. Levinger, and P. F. Barbara, *J. Phys. Chem.*, **98**, 1228 (1993).
- 2 A. N. Macpherson, P. A. Liddell, S. Lin, L. Noss, G. R. Seely, J. M. DeGraziano, A. L. Moore, T. A. Moore, and D. Gust, *J. Am. Chem. Soc.*, **117**, 7202 (1995).
- 3 T. Häberle, J. Hirsch, F. Pöllinger, H. Heitele, M. E. Michel-Beyerle, C. Anders, A. Döhling, C. Krieger, A. Rühckemann, and H. A. Staab, *J. Phys. Chem.*, **100**, 18269 (1996).
- 4 P. F. Barbara, T. J. Meyer, and M. A. Ratner, *J. Phys. Chem.*, **100**, 13148 (1996).
- 5 H. Kido, H. Nagino, and T. Ito, *Chem. Lett.*, **1996**, 745.
- 6 T. Sakuma, H. Kido, "Abstracts of 31st International Conference on Coordination Chemistry," Vancouver (1996).
- 7 T. Ito, T. Hamaguchi, H. Nagino, T. Yamaguchi, J. Washington, and C. Kubriak, *Science*, **277**, 660 (1997).
- 8 N. Tamai, T. Yamazaki, and I. Yamazaki, *Can. J. Phys.*, **68**, 1013 (1990).
- 9 S. Akimoto, S. Takaichi, T. Ogata, Y. Nishimura, I. Yamazaki, and M. Mimuro, *Chem. Phys. Lett.*, **260**, 147 (1996).
- 10 M. Mimuro, S. Akimoto, S. Takaichi, and I. Yamazaki, *J. Am. Chem. Soc.*, **119**, 1452 (1997).
- 11 Th. Förster, *Discuss. Faraday Soc.*, **27**, 7 (1959).
- 12 J. A. Baumann, D. J. Salmon, S. T. Wilson, T. J. Meter, and W. E. Hatfield, *Inorg. Chem.*, **17**, 3342 (1978).
- 13 R. A. Marcus and N. Sutin, *Biochim. Biophys. Acta*, **811**, 265 (1985).
- 14 P. Siders and R. A. Marcus, *J. Am. Chem. Soc.*, **103**, 748 (1981).
- 15 T. Asahi, M. Ohkohchi, R. Matsusaka, N. Mataga, R. P. Zhang, A. Osuka, and K. Maruyama, *J. Am. Chem. Soc.*, **115**, 5665 (1993).
- 16 A. Mokhtari, J. Chesnoy, and A. Laubereau, *Chem. Phys. Lett.*, **155**, 593 (1989).
- 17 I. Martini and G. V. Hartland, *J. Phys. Chem.*, **100**, 19764 (1996).